J Bioenerg Biomembr (2008) 40:475–483
DOI 10.1007/s10863-008-9171-9

Challenges in elucidating structure and mechanism of proton pumping NADH:ubiquinone oxidoreductase (complex I)

Volker Zickermann · Stefan Dröse · Maja A. Tocilescu · Klaus Zwicker · Stefan Kerscher · Ulrich Brandt

Received: 3 July 2008 / Accepted: 1 August 2008 / Published online: 4 November 2008

Abstract Proton pumping NADH:ubiquinone oxidoreductase (complex I) is the most complicated and least understood enzyme of the respiratory chain. All redox prosthetic groups reside in the peripheral arm of the L-shaped structure. The NADH oxidation domain harbouring the FMN cofactor is connected via a chain of iron–sulfur clusters to the ubiquinone reduction site that is located in a large pocket formed by the PSST- and 49-kDa subunits of complex I. An access path for ubiquinone and different partially overlapping inhibitor binding regions were defined within this pocket by site directed mutagenesis. A combination of biochemical and single particle analysis studies suggests that the ubiquinone reduction site is located well above the membrane domain. Therefore, direct coupling mechanisms seem unlikely and the redox energy must be converted into a conformational change that drives proton pumping across the membrane arm. It is not known which of the subunits and how many are involved in proton translocation. Complex I is a major source of reactive oxygen species (ROS) that are predominantly formed by electron transfer from $FMNH_2$. Mitochondrial complex I can cycle between active and deactive forms that can be distinguished by the reactivity towards divalent cations and thiol-reactive agents. The physiological role of this phenomenon is yet unclear but it could contribute to the regulation of complex I activity *in-vivo*.

V. Zickermann · S. Dröse · M. A. Tocilescu · K. Zwicker · S. Kerscher · U. Brandt (✉)
Goethe-Universität, Fachbereich Medizin, Molekulare Bioenergetik, Cluster of Excellence Frankfurt, Macromolecular Complexes, ZBC, Theodor-Stern-Kai 7, Haus 26, 60590 Frankfurt am Main, Germany
e-mail: brandt@zbc.kgu.de

Keywords Complex I · NADH dehydrogenase · NDH-1 · Mitochondria · Proton pumping · Ubiquinone · Superoxide · Iron–sulfur cluster · Active/deactive transition · Electron microscopic single particle analysis

Introduction

In his Nobel-Lecture Peter Mitchell defined the three central questions to be answered about all chemiosmotic systems (Mitchell 1979): What is it? What does it do? How does it do it? Despite of some remarkable progress made, we have to recognize 30 years later that for proton pumping NADH:ubiquinone oxidoreductase (complex I) of the respiratory chain—if at all—we have just answered the first two question. Clearly this is due to the fact that complex I is very large and has numerous subunits and redox centres (Brandt 2006). It contains a core of 14 subunits that are conserved in prokaryotes and eukaryotes and comprises eight to nine iron–sulfur clusters and one FMN. Seven of these subunits are encoded by the mitochondrial genome in most eucaryotes and form the common membrane integral part of complex I. Up to 31 additional 'accessory' subunits are found in mitochondrial versions of complex I (Morgner et al. 2008; Cardol et al. 2004; Carroll et al. 2006).

Regarding the second question, the overall reaction catalyzed is well established, at least for the mitochondrial enzyme:

$$\mathrm{NADH} + \mathrm{ubiquinone} + 5\mathrm{H}^{+}_{\mathrm{Matrix}} \rightarrow \mathrm{NAD}^{+} + \mathrm{ubiquinol} + 4\mathrm{H}^{+}_{\mathrm{Intermembrane\ space}}$$

In the presence of a protonmotive force this reaction can be reversed. It is also well established that complex I

contributes significantly to cellular oxidative stress and possibly redox-signaling by the generation of superoxide. However, it remains unclear if and how the accessory subunits of complex I may take part in additional metabolic routes as suggested e.g. by the presence of a mitochondrial acyl carrier protein subunit, containing phosphopantethein (Runswick et al. 1991) and a NADPH binding site in the 39-kDa accessory subunit (Abdrakhmanova et al. 2006; Schulte et al. 1999).

No definite answers can be given to the third question. Most importantly, the central chemisosmotic question of how electron transport is linked to vectorial proton translocation in complex I remains unanswered so far. However, structural and functional data obtained in recent years have imposed important constraints that limit the number of possible mechanisms by excluding most of the hypothetical models that were proposed over the years. In this sense, the complex I field has been following another most valuable advice given by Peter Mitchell (Mitchell 1979): "Conjectures about direct biochemically explicit chemiosmotic mechanisms, on the other hand, even if wrong, promote experimental activity and enthusiasm by suggesting crucial experiments for testing them."

The aim of this short review is to highlight the most important progress that has been made in elucidating the structural organization and functional framework of complex I. This will define a number of key issues that are in the current focus of the field.

Overall architecture of complex I

An L-shaped architecture of complex I from different organisms was observed by electron microscopy. Both arms have approximately the same size. In the most detailed structure of the holoenzyme obtained for complex I from *Yarrowia lipolytica*, distinct structural features and subdomains can be discerned in the membrane and the peripheral arm (Radermacher et al. 2006). The additional proteins of the mitochondrial enzyme seem to be grouped around a central core common to prokaryotic and eukaryotic complexes (Guenebaut et al. 1998). Functionally, complex I can be subdivided into three modules (Brandt 2006) of different evolutionary origin (Friedrich and Weiss 1997). Two of them, the N- and the Q-modules, form the peripheral arm of complex I that protrudes into the mitochondrial matrix or the bacterial cytoplasm and contains all known redox-prosthetic groups. The relative positions of its core subunits and redox centres are known in detail from the X-ray structure of the peripheral arm of the bacterial complex from *Thermus thermophilus* (Sazanov and Hinchliffe 2006). The N-module contains the binding site for the substrate NADH and for FMN in the 51-kDa subunit (The subunit nomenclature for bovine complex I will be used throughout). The same subunit contains the tetranuclear iron–sulfur cluster N3 which is the first in a "wire" of seven clusters leading to the ubiquinone binding site (Fig. 1). This wire does not include binuclear iron–sulfur cluster N1a residing on the opposite side of FMN in the adjacent 24–kDa subunit. Two tetranuclear and one binuclear iron–sulfur cluster bound to the 75-kDa subunit guide the electrons to the Q-module. There, three tetranuclear clusters of the TYKY- and the PSST- subunit form the

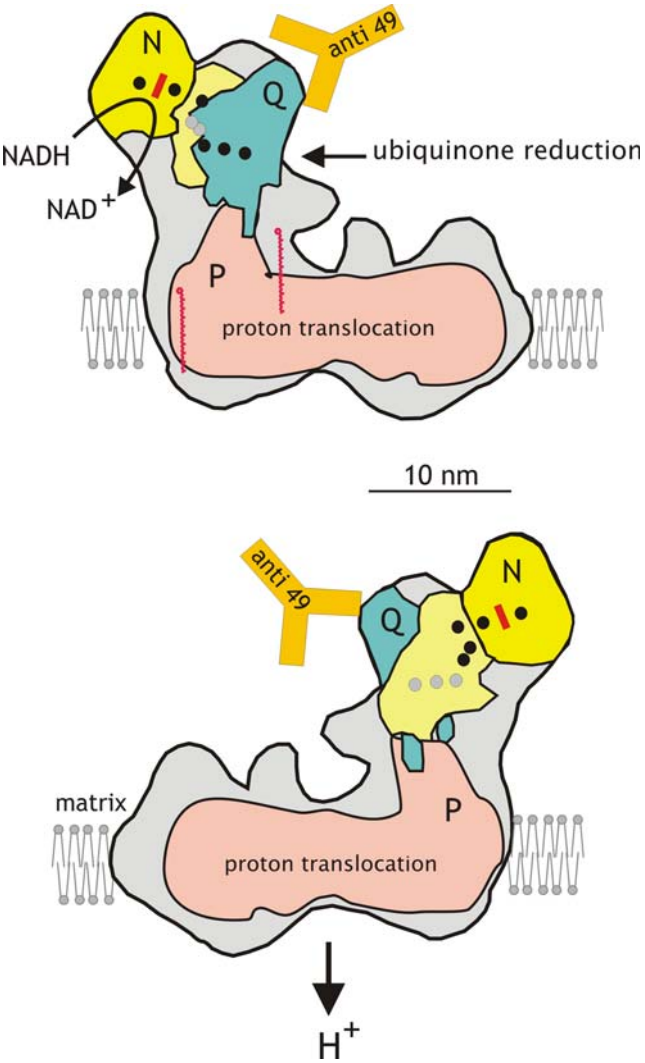

Fig. 1 Two views of the proposed overall architecture of complex I. Complex I consists of three functional modules: *N* (NADH oxidation, *yellow*), *Q* (ubiquinone reduction, *blue-green*) and *P* (proton pumping, *light red*). The architecture of the peripheral arm corresponds to fit 1 from (Clason et al. 2007). The binding region of an antibody against the 49-kDa subunit of the Q module is indicated by an *orange Y*. The mass corresponding to the 51-kDa and 24-kDa subunits missing in a subcomplex analyzed by single particle analysis (Clason et al. 2007) is depicted in *a darker shade of yellow*. Iron–sulfur centers are shown as *black* and *grey* (if hidden) *circles*. Ubiquinone molecules in an extended conformation are drawn to scale in *red*. The *red bar* indicates the approximate position of FMN

end of a ~90 Å long electron transfer chain where ubiquinone gets reduced (see below). The 49-kDa and the 30-kDa subunit do not contain prosthetic groups, but are also part of the Q-module. Iron–sulfur cluster N2—the last in the chain—resides at the interface between the 49-kDa subunit and the PSST subunit that contains its ligands.

Much less is known about the P-module that consists of the remaining seven, membrane integral core subunits und must contain the proton translocation machinery.

Assignment of iron–sulfur clusters

The structure of the peripheral arm of complex I from *T. thermophilus* revealed nine iron–sulfur clusters consistent with the number of binding motifs found in its subunits (Sazanov and Hinchliffe 2006). Based on a series of previous spectroscopic, biochemical and mutational studies (Ohnishi 1998) EPR-signals were assigned to the individual clusters seen in the X-ray structure (Sazanov and Hinchliffe 2006), but some aspects of this assignment were recently challenged (Yakovlev et al. 2007).

Reduced bi- and tetranuclear iron–sulfur clusters are paramagnetic and can be analyzed by cw-EPR spectroscopy. However, of the eight iron–sulfur clusters present in mitochondrial complex I, only six individual spectra could be distinguished so far in isolated complex I from bovine heart mitochondria. These EPR signals were named N1a, N1b, N2, N3, N4, N5 according to their increasing spin relaxation rate (Ohnishi 1998). Slow spin relaxation identifies N1a and N1b as binuclear [2Fe–2S] clusters. The other signals originate from fast relaxing tetranuclear [4Fe–4S] clusters. It is unclear why the remaining two clusters are not detectable. This might be due to very low redox potentials resulting in an oxidised diamagnetic state or more likely, to very fast spin relaxation rates which prevent detection by cw-EPR spectroscopy. There is consensus about the identity of iron–sulfur clusters N1a, N2 and N3. In addition, the second binuclear cluster bound to the 75-kDa subunit must correspond to EPR signal N1b. Of the remaining four binding motifs two are located in the TYKY- and two in the 75-kDa subunit. However, the assignment of the remaining two EPR signals (N4 and N5) and the identity of the two EPR silent iron–sulfur clusters are under debate (Ohnishi and Nakamaru-Ogiso 2008; Yakovlev et al. 2007). It is beyond the scope of this review to discuss the details of this controversy, however the underlying problems can be illustrated by the following example: Based on mutational studies with the heterologously expressed 75-kDa subunit of *Paracoccus denitrificans* EPR signal N5 was attributed to the binding motif comprising three cysteines and one histidine (Yano et al. 2003). However this result could not be confirmed because exchange of the histidine ligand in complex I from *Y. lipolytica* did not change the EPR signature of iron–sulfur cluster N5 (Waletko et al. 2005).

Evidently, the available biochemical and spectroscopic data from subcomplexes, heterologously expressed subunits and mutational studies are not sufficient to unambiguously assign the cw-EPR spectra N4 and N5 to a specific cluster in the structure. One approach that may help to solve this problem is the separation of paramagnetic species based on differences in their relaxation behaviour by pulsed EPR techniques (Maly et al. 2004). T1 and T2 relaxation rates can be used to obtain separate spectra of individual iron–sulfur clusters (Cernescu et al. 2008). Dipolar coupling affects T2 relaxation behaviour and can be employed to obtain information on the spatial arrangement in relation to the paramagnetic neighbours of an iron–sulfur cluster. A fast relaxing cluster in the neighbourhood, even if this cluster is invisible in cw-EPR, might be assigned indirectly by analysing its effects on relaxation properties of an EPR detectable cluster. This should yield a more complete assignment of clusters identified in the partial structure of complex I to the corresponding EPR spectra.

Orientation of the peripheral arm

As such, the X-ray structure of the peripheral arm provides no clear information on how it is oriented relative to the membrane arm of complex I. At first sight it seems obvious that iron–sulfur cluster N2 should be located as close as possible to the membrane interface to allow the electrons to reach the highly hydrophobic substrate ubiquinone (Sazanov and Hinchliffe 2006). However, this notion is not supported by studies using a combination of protein chemistry and the electron microscopy structure of complex I from *Y. lipolytica*. Single particle analysis of complex I decorated with antibodies directed against the 49-kDa and the 30-kDa subunit suggests that the corresponding epitopes in these subunits of the Q module reside at a considerable distance from the membrane arm (Zickermann et al. 2003). Moreover, a 3D reconstruction of a subcomplex lacking specifically the flavoprotein part of the N-module (Zickermann et al. 2007) clearly indicated a position of the 51-kDa and 24-kDa subunits at the very distal end of the peripheral arm (Clason et al. 2007). This assignment could be used as an anchor point to fit the X-ray structure of the peripheral arm fragment from *T. thermophilus* into the electronmicroscopic structure of complex I from *Y. lipolytica*. Due to the presence of extra domains from the additional accessory subunits of the mitochondrial enzyme the orientation could not be determined unambiguously. However, none of the possible orientations placed iron–sulfur cluster N2 closer than 35 Å to the membrane arm. Several orientations could

be excluded simply because shielding of an epitope in the 49-kDa subunit would prevent interaction with monoclonal antibodies known to bind to the intact complex. The combination of evidence for subcomplex and antibody labelling studies results in a clear preference for the orientation shown in Fig. 1. According to this arrangement, the 49-kDa subunit resides in the middle of the peripheral arm placing iron–sulfur cluster N2 about 60 Å above the membrane domain. This unexpected situation poses two questions: What bridges the gap between Q-module and membrane domain of complex I and how do the electrons reach the hydrophobic substrate ubiquinone?

In the proposed orientation of the peripheral arm helix H1 of the PSST subunit (Fig. 2) extends towards the membrane arm, but it is insufficient to form the connection between iron–sulfur cluster N2 and the membrane interface. Additional contributions could come from 34 N-terminal amino acids of the 49-kDa subunit and 32 amino acids at the N-terminus and an internal loop of the PSST subunit that are disordered in the X-ray structure of the peripheral arm (Sazanov and Hinchliffe 2006). To fill the gap regions from other proteins are clearly needed that can only come from the membrane integral subunits of the P-module. One candidate is the ND3 subunit that could be cross-linked with the PSST and 49-kDa subunits (Kao et al. 2004b). Subunit ND3 is a largely hydrophobic 15 kDa protein with three predicted transmembrane helices of which two are connected by a loop of about 25 amino acids. However, the topology of subunit ND3 and therefore the location of this loop is controversially discussed (Di Bernardo et al. 2000; Galkin et al. 2008). The fact that several pathogenic mutations were reported in this loop (McFarland et al. 2004; Sarzi et al. 2007) and the identification of a cysteine in this loop as the one specifically exposed only in deactive complex I (Galkin et al. 2008) argues for its orientation towards the peripheral arm where it could contribute to the connection to the Q-module. Additional contributions could come from subunit ND1 since changes in the kinetic parameters of ubiquinone reductase activity of mutants in a predicted surface helix of the ND1 subunit were reported (Zickermann et al. 1998). It should also be noted that the prediction of transmembrane helices has proven to be unreliable in some cases. Therefore it cannot be excluded that some segments of the membrane integral subunits of complex I assumed to cross the membrane, may take part in forming the stalk connecting the P- and the Q-module. A rather hydrophobic or amphipathic character of this region of complex I would also seem attractive to answer the second question: One option to solve the problem that iron–sulfur cluster N2 is too far up in the peripheral arm to reduce ubiquinone in the membrane would be that the hydrophobic substrate would diffuse out of the membrane domain to reach its reductant. This would call for a hydrophobic or amphipathic ramp or channel in the connecting region. The only other option would be that large scale conformational changes could bring cluster N2 close enough to the membrane domain during turnover to reduce ubiquinone.

Quinone and inhibitor binding pocket

Paramagnetic coupling between ubisemiquinone and reduced iron–sulfur cluster N2 indicating a distance of 8–12 Å was observed during steady state turnover of bovine heart complex I (Vinogradov et al. 1995). A large pocket in the X-ray structure of the peripheral arm of complex I from *T. thermophilus* reaching the vicinity of iron–sulfur cluster N2 suggested that this semiquinone is indeed a substrate intermediate. A large number of mutations had differential effects on ubiquinone reductase activity allowing the assignment of functional domains in the quinone binding pocket (Fig. 2; Tocilescu et al. 2007). Mutations in a stretch of about 25 Å reaching from a three-stranded β-sheet at the N-terminus of the 49-kDa subunit to Tyrosine 144 next to iron–sulfur cluster N2 in all cases drastically reduced complex I activity suggesting that the corresponding residues may contribute to an entry path leading the substrate molecule to its active site. It should be noted that the middle strand of this β-sheet had been identified as the epitope for one of the monoclonal antibodies used in the localization studies discussed above (Fig. 2; Zickermann et al. 2003). This indicates that the opening of the substrate binding pocket must be exposed to the bulk phase in intact complex I. Exchanges deeper in the pocket result in a moderate decrease of complex I activity depending on the nature of the introduced residue. Interestingly, mutagenesis of some strongly conserved amino acids lining a narrow gorge at the distal end of the quinone binding pocket was found to have no effect on complex I activity (Tocilescu et al. 2007).

A large number of chemically diverse compounds blocks ubiquinone reduction by complex I. Based on their kinetic characteristics in steady state inhibition kinetics, they were subdivided into three classes (Degli Esposti 1998). Inhibitor binding studies indicated that compounds from all three classes exhibit different but partially overlapping binding sites in a common binding pocket (Okun et al. 1999). Extensive mutagenesis studies of the 49-kDa and PSST subunits of complex I from *Rhodobacter capsulatus* (Darrouzet et al. 1998; Prieur et al. 2001) and *Y. lipolytica* (Fendel et al. 2008; Grgic et al. 2004; Kashani-Poor et al. 2001; Tocilescu et al. 2007) confirmed this result and revealed that these binding sites, like the ubiquinone access path, are located in the large pocket next to iron–sulfur cluster N2 (Fig. 2). Mutation of positions which resulted in changed I_{50} for rotenone (class B inhibitor) in all cases had

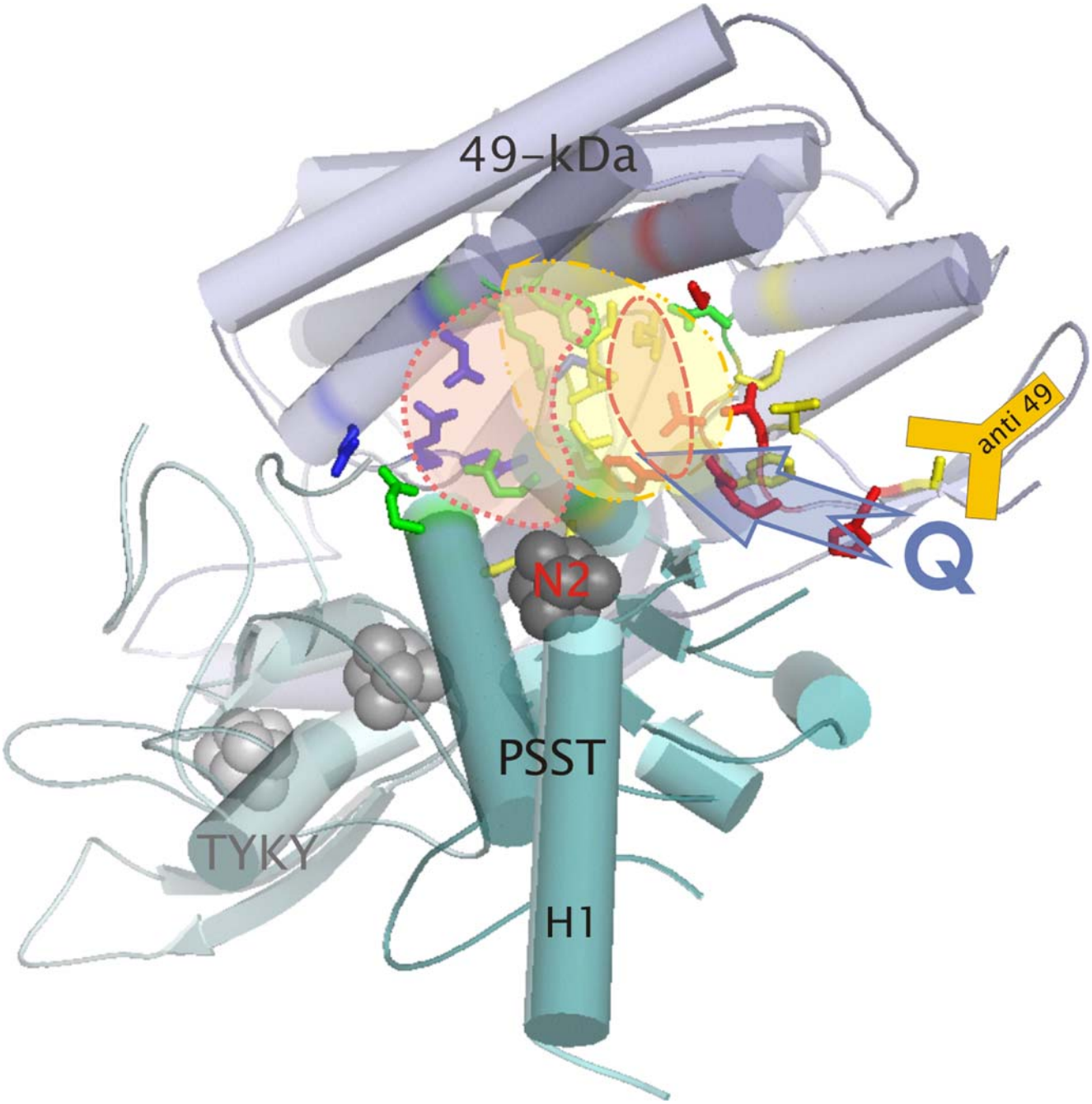

Fig. 2 Ubiquinone access path and inhibitor binding regions. Cartoon of the structure of the PSST- (*cyan*), 49-kDa (*blue*) and TYKY- (*grey*) subunits (Sazanov and Hinchliffe 2006) shown in an orientation similar to the one in *top panel* of Fig. 1. The three iron–sulfur clusters of the Q module are shown as space-fill models. Amino acid residues lining the quinone binding pocket are shown as *stick models* and color coded as follows: *red*, all of several exchanges resulted in very low activity (<25% of parental); *yellow*, at least one exchange resulted in very low activity (<25% of parental); *green*, reduced activity (between 25% and 75% of parental); *blue*, essentially normal activity (>75% of parental) for all exchanges. The binding regions for the different inhibitor classes are illustrated by *coloured areas*: ....(*ruby-red*), $C_{12}E_8$; -·· (*yellow*), rotenone and DQA, - - - - (*orange-red*), DQA only. The location of the epitope for the anti 49-kDa antibody is indicated by an *orange Y*

effects on the I_{50} of DQA (class A inhibitor) and clustered in a region corresponding to the former [NiFe]-binding fold in homologous [NiFe] hydrogenases (Kerscher et al. 2001). However, mutations which had an effect on the I_{50} of DQA only were located deeper in the 49-kDa subunit. Effects on the I_{50} of the class C inhibitor $C_{12}E_8$ were found in a narrow gorge at the distal end of the pocket. Consistently, mutations on some exposed positions resulted in changed I_{50} values for inhibitors from all three classes (Fendel et al. 2008). In line with these results the PSST subunit was also

by photoaffinity labelling shown to be a major contributor to the inhibitor binding site (Nakamaru-Ogiso et al. 2003; Schuler et al. 1999).

Localization of the proton pumping site

Proton pumping by complex I with a stoichiometry of 4 H^+ per NADH oxidized contributes a major portion to the proton motive force that drives ATP synthesis (Galkin et al. 2006; Wikström 1984). From the discussion in the previous chapters it is evident that the redox chemistry of complex I takes place exclusively in the peripheral arm. This renders previously proposed direct coupling mechanisms unlikely (Brandt 1997; Dutton et al. 1998) and rather implies that the driving force for proton translocation must be transduced over a considerable distance to the actual pumping process in the P-module via conformational coupling (Brandt et al. 2003; Friedrich 2001). In fact, evidence for structural changes upon reduction of complex I by NADH were obtained by cross linking studies (Belogrudov and Hatefi 1994; Mamedova et al. 2004) and differential susceptibility to proteolytic degradation (Yamaguchi et al. 1998).

It follows that two separate processes connected by conformational coupling have to be analyzed to elucidate the proton pumping mechanism of complex I. The first process to understand is the chemistry of the controlled conversion of redox energy into conformational energy taking place in the peripheral arm; the second are the steps leading to gated proton translocation across the membrane domain.

Simulations (Moser et al. 2006) and fast kinetics (Verkhovskaya et al. 2008) indicate that electrons flow rapidly from FMN all the way to iron–sulfur cluster N2 suggesting that the energy converting reaction occurs at this cluster or further downstream during ubiquinone reduction. Iron–sulfur cluster N2 has the highest midpoint potential of all redox centers and exhibits a pronounced pH dependence of its redox potential (Ohnishi 1998). Based on these properties several mechanistic models had been proposed assigning a key role in proton translocation to this redox centre (Brandt 1999; Ohnishi and Salerno 2005). However, when a histidine of the 49-kDa subunit that is located in the immediate vicinity of iron–sulfur cluster N2 was mutated to methionine in *Y. lipolytica* this completely abolished pH dependence and shifted the midpoint potential by −140 mV at pH 6.0 (Zwicker et al. 2006). Yet this did not significantly affect the ubiquinone reductase activity and there was no change in proton pumping stoichiometry. Thus it seems most likely that the conformational change that drives proton translocation in the P-module is linked exclusively to the chemistry of ubiquinone reduction.

The actual proton translocating machinery must be located in one or several of the seven central hydrophobic subunits forming the P-module (subunits ND1-ND6 and ND4L). However it remains to be established how many pump sites there are in complex I and which subunits of the P module are actually involved in proton translocation. Subunits ND2, ND4 and ND5 exhibit some homology to sodium proton antiporters and were therefore proposed to be part of the proton pumping machinery of complex I (Mathiesen and Hägerhall 2002). A 3D structure of the membrane arm of complex I from *Escherichia coli* at 8 Å resolution has been obtained by electron microscopy of 2D crystals (Baranova et al. 2007a). Subunits ND4 and ND5 that are the two largest of the membrane integral central subunits were shown to reside at the distal end of the membrane arm (Baranova et al. 2007b; Holt et al. 2003).

Charged residues in putative transmembrane regions were found in several hydrophobic subunits. A number of mutants in hydrophobic subunits has been generated and investigated including subunit ND1 (Kurki et al. 2000), subunit ND3 (Kao et al. 2004a), subunit ND4L (Kao et al. 2005b; Kervinen et al. 2004), subunit ND4 (Euro et al. 2008; Torres-Bacete et al. 2007), and subunit ND6 (Kao et al. 2005a). Remarkably many of the mutations affected ubiquinone reductase activity. Rather than indicating a contribution of hydrophobic subunits to ubiquinone binding this probably reflects the fact that redox chemistry and proton pumping must be tightly coupled. At present it is impossible to draw any firm conclusions on the involvement of individual subunits of the P-module in the proton pumping activity of complex I.

ROS production by complex I

Within the respiratory chain, complex I and the cytochrome bc_1 complex (complex III, ubiquinol:cytochrome *c* oxidoreductase) were identified as the main sources of 'reactive oxygen species' (ROS; Fridovich 1978; Turrens 2003). While complex III produces superoxide preferably under conditions of 'oxidant-induced-reduction', i.e. in the presence of the specific centre N inhibitor antimycin A, with sufficient amounts of reducing equivalents and an oxidized downstream respiratory chain, complex I was shown to generate superoxide under specific circumstances at high rates in the absence of inhibitors. Hence, most groups working in the ROS-field regard complex I as the more important mitochondrial source of deleterious ROS. All major cofactors involved in the electron transfer chain have been proposed as the source of superoxide: the flavin (Galkin and Brandt 2005; Kussmaul and Hirst 2006; Liu et al. 2002; Vinogradov and Grivennikova 2005), iron-sulfur clusters N2 (Genova et al. 2001) and N1a (Kushnareva et al. 2002), and a semiquinone radical that is formed upon ubiquinone reduction (Lambert and Brand 2004a; Ohnishi

et al. 2005). Even an enzyme-bound NAD radical has been considered as a possible electron source for superoxide production (Krishnamoorthy and Hinkle 1988). Although contributions from other redox centers cannot be fully excluded at present, it seems clear now that reduced FMN is the major source of electrons for ROS formation in complex I (Galkin and Brandt 2005; Kussmaul and Hirst 2006). For mammalian complex I it was shown that superoxide anion radicals ($O_2^{\bullet -}$) are the main ROS delivered by complex I (Kussmaul and Hirst 2006). In contrast, bacterial complex I seems to produce mainly H_2O_2 during the direct reduction of O_2 (Esterhazy et al. 2008). This difference may be due to the marked difference in the redox potential of iron–sulfur cluster N1a that is much more negative in the mitochondrial enzyme.

In intact mitochondrial membranes superoxide production by complex I can be stimulated in two different ways (Kushnareva et al. 2002; Lambert and Brand 2004a; Liu et al. 2002; Votyakova and Reynolds 2001). In mitochondria respiring on NADH-generating substrates (e.g. malate/glutamate or malate/pyruvate) superoxide production is low and increases with inhibitors blocking downstream electron transfer due to a higher degree of reduction of the redox cofactors of complex I including FMN. The highest rates of superoxide production are measured under conditions of succinate-supported reverse electron transfer from complex II via ubiquinone and complex I onto NAD^+ (Hinkle et al. 1967; Vinogradov and Grivennikova 2005; Votyakova and Reynolds 2001). Under these conditions the redox centers of complex I are even more reduced, but this state and therefore ROS formation is now highly sensitive to even a small drop in the protonmotive force, and interestingly, the ΔpH component seems to be the main determinant (Lambert et al. 2008; Lambert and Brand 2004b).

Active/deactive transition of complex I

It is known for many years that complex I can undergo an active/deactive (A/D) transition (overview in Vinogradov 1998). Exposure of complex I to elevated temperature in the absence of substrates results in transition to the D-form that is characterized by a considerable lag phase of the NADH:ubiquinone oxidoreductase activity. Bivalent cations (like Ca^{2+}) and alkaline pH accelerate the A to D transition. The lag phase is abolished by incubation of the enzyme under conditions that allow catalytic turnover, thus providing 'reactivation' of the enzyme. A cysteine residue in a 15 kDa protein was found to be modified by *N*-ethyl malemide selectively only in the D-, but not in the A-from of bovine heart complex I (Gavrikova and Vinogradov 1999). Modification of this cysteine inhibits complex I activity probably by preventing its transition to the A-form. Inhibition by this mechanism is also observed following selective nitrosation of the D-form with peroxynitrite and a pathophysiological significance of this modification during sepsis has been proposed (Galkin and Moncada 2007). So far, A/D transition has been observed with eukaryotic complex I from vertebrates and fungi (Maklashina et al. 2003). It has been suggested that this phenomenon might be associated with one of the accessory subunits not present in bacteria and that this subunit contained the cysteine residue only accessible in the D-form. However recently the residue was identified in bovine heart complex I as Cys-39 of the central ND3 subunit also present in the bacterial enzyme (Galkin et al. 2008). Interestingly, the highly conserved residue is replaced by serine in *E. coli* and *T. thermophilus*. However, not all eukaryotes that show A/D-transition contain this cysteine, suggesting that it is not required for this process. Rather its accessibility can be taken as an indicator for the functional transition of complex I. The physiological significance of the A/D-transition remains to be established.

Conclusions

Although recent work has provided many insights into the composition and overall architecture of complex I, we have only just started to understand what it does. The physiological role of additional functional aspects of complex I like ROS formation and active/deactive transition is only poorly understood. Even less is known about how complex I works. Even its core bioenergetic function, the mechanism of redox linked proton pumping is still elusive. However, in contrast to the direct chemiosmotic mechanisms envisioned by Peter Mitchell for "phase 1" or "coupling site I" of the respiratory chain, it seems inevitable to conclude that redox chemistry drives proton translocation via a conformational mechanism. Clearly a high-resolution structure of the entire complex I and explicit models for the redox-chemistry involved in energy conversion are needed to avoid the potential problems foreseen by Peter Mitchell in this situation: "By providing a blanket explanation, but without currently testable detail, it seems to me that the concept of exclusively conformational coupling in chemiosmotic reactions...may actually inhibit productive research by acting as a palliative (Mitchell 1979)."

References

Abdrakhmanova A, Zickermann K, Kerscher S, Zickermann V, Brandt U (2006) Biochim Biophys Acta 1757:1676–1682

Baranova EA, Holt PJ, Sazanov LA (2007a) J Mol Biol 366:140–154
Baranova EA, Morgan DJ, Sazanov LA (2007b) J Struct Biol 159:238–242
Belogrudov G, Hatefi Y (1994) Biochemistry 33:4571–4576
Brandt U (1997) Biochim Biophys Acta 1318:79–91
Brandt U (1999) BioFactors 9:95–101
Brandt U (2006) Annu Rev Biochem 75:69–92
Brandt U, Kerscher S, Dröse S, Zwicker K, Zickermann V (2003) FEBS Lett 545:9–17
Cardol P, Vanrobaeys F, Devreese B, Van Beeumen J, Matagne RF, Remacle C (2004) Biochim Biophys Acta 1658:212–224
Carroll J, Fearnley IM, Skehel JM, Shannon RJ, Hirst J, Walker JE (2006) J Biol Chem 281:32724–32727
Cernescu A, Maly T, Prisner TF (2008) J Magn Reson 192:78–84
Clason T, Zickermann V, Ruiz T, Brandt U, Radermacher M (2007) J Struct Biol 159:433–442
Darrouzet E, Issartel JP, Lunardi J, Dupuis A (1998) FEBS Lett 431: 34–38
Degli Esposti M (1998) Biochim Biophys Acta 1364:222–235
Di Bernardo S, Yano T, Yagi T (2000) Biochemistry 39:9411–9418
Dutton PL, Moser CC, Sled VD, Daldal F, Ohnishi T (1998) Biochim Biophys Acta 1364:245–257
Esterhazy D, King MS, Yakovlev G, Hirst J (2008) Biochemistry 47:3964–3971
Euro L, Belevich G, Verkhovsky MI, Wikström M, Verkhovskaya M (2008) Biochim Biophys Acta 1777:1166–1172
Fendel U, Tocilescu MA, Kerscher S, Brandt U (2008) Biochim Biophys Acta (BBA)—Bioenerg 1777:660–665
Fridovich I (1978) Science 201:875–880
Friedrich T (2001) J Bioenerg Biomembr 33:169–177
Friedrich T, Weiss H (1997) J Theor Biol 187:529–540
Galkin A, Brandt U (2005) J Biol Chem 280:30129–30135
Galkin A, Moncada S (2007) J Biol Chem 282:37748–37753
Galkin A, Dröse S, Brandt U (2006) Biochim Biophys Acta 1757:1575–1581
Galkin A, Meyer B, Wittig I, Karas M, Schägger H, Vinogradov AD, Brandt U (2008) J Biol Chem 283:20907–20913
Gavrikova EV, Vinogradov AD (1999) FEBS Lett 455:36–40
Genova ML, Ventura B, Giuliano G, Bovina C, Formiggini G, Parenti Castelli G, Lenaz G (2001) FEBS Lett 505:364–368
Grgic L, Zwicker K, Kashani-Poor N, Kerscher S, Brandt U (2004) J Biol Chem 279:21193–21199
Guenebaut V, Schlitt A, Weiss H, Leonard K, Friedrich T (1998) J Mol Biol 276:105–112
Hinkle PC, Butow RA, Racker E, Chance B (1967) J Biol Chem 242:5169–5173
Holt PJ, Morgan DJ, Sazanov LA (2003) J Biol Chem 278:43114–43120
Kao MC, Di Bernardo S, Perego M, Nakamaru-Ogiso E, Matsuno-Yagi A, Yagi T (2004a) J Biol Chem 279:32360–32366
Kao MC, Matsuno-Yagi A, Yagi T (2004b) Biochemistry 43:3750–3755
Kao MC, Di Bernardo S, Nakamaru-Ogiso E, Miyoshi H, Matsuno-Yagi A, Yagi T (2005a) Biochemistry 44:3562–3571
Kao MC, Nakamaru-Ogiso E, Matsuno-Yagi A, Yagi T (2005b) Biochemistry 44:9545–9554
Kashani-Poor N, Zwicker K, Kerscher S, Brandt U (2001) J Biol Chem 276:24082–24087
Kerscher S, Kashani-Poor N, Zwicker K, Zickermann V, Brandt U (2001) J Bioenerg Biomembr 33:187–196
Kervinen M, Patsi J, Finel M, Hassinen IE (2004) Biochemistry 43:773–781
Krishnamoorthy G, Hinkle PC (1988) J Biol Chem 263:17566–17575
Kurki S, Zickermann V, Kervinen M, Hassinen IE, Finel M (2000) Biochemistry 39:13496–13502
Kushnareva Y, Murphy AN, Andreyev A (2002) Biochem J 368: 545–553
Kussmaul L, Hirst J (2006) Proc Natl Acad Sci U S A 103:7607–7612
Lambert AJ, Brand MD (2004a) J Biol Chem 279:39414–39420
Lambert AJ, Brand MD (2004b) Biochem J 382:511–517
Lambert AJ, Buckingham JA, Brand MD (2008) FEBS Lett 582:1711–1714
Liu Y, Fiskum G, Schubert D (2002) J Neurochem 80:780–787
Maklashina E, Kotlyar AB, Cecchini G (2003) Biochim Biophys Acta 1606:95–103
Maly T, MacMillan F, Zwicker K, Kashani-Poor N, Brandt U, Prisner TF (2004) Biochemistry 43:3969–3978
Mamedova AA, Holt PJ, Carroll J, Sazanov LA (2004) J Biol Chem 279:23830–23836
Mathiesen C, Hägerhall C (2002) Biochim Biophys Acta 1556: 121–132
McFarland R, Kirby DM, Fowler KJ, Ohtake A, Ryan MT, Amor DJ, Fletcher JM, Dixon JW, Collins FA, Turnbull DM, Taylor RW, Thorburn DR (2004) Ann Neurol 55:58–64
Mitchell P (1979) Science 206:1148–1159
Morgner N, Zickermann V, Kerscher S, Wittig I, Abdrakhmanova A, Barth HD, Brutschy B, Brandt U (2008) Biochim Biophys Acta (in press)
Moser CC, Farid TA, Chobot SE, Dutton PL (2006) Biochim Biophys Acta—Bioenerg 1757:1096–1109
Nakamaru-Ogiso E, Sakamoto K, Matsuno-Yagi A, Miyoshi H, Yagi T (2003) Biochemistry 42:746–754
Ohnishi T (1998) Biochim Biophys Acta 1364:186–206
Ohnishi T, Nakamaru-Ogiso E (2008) Biochim Biophys Acta 1777:703–710
Ohnishi T, Salerno JC (2005) FEBS Lett 579:4555–4561
Ohnishi T, Johnson JE Jr, Yano T, LoBrutto R, Widger WR (2005) FEBS Lett 579:500–506
Okun JG, Lümmen P, Brandt U (1999) J Biol Chem 274:2625–2630
Prieur I, Lunardi J, Dupuis A (2001) Biochim Biophys Acta 1504: 173–178
Radermacher M, Ruiz T, Clason T, Benjamin S, Brandt U, Zickermann V (2006) J Struct Biol 154:269–279
Runswick MJ, Fearnley IM, Skehel JM, Walker JE (1991) FEBS Lett 286:121–124
Sarzi E, Brown MD, Lebon S, Chretien D, Munnich A, Rotig A, Procaccio V (2007) Am J Med Genet A 143:33–41
Sazanov LA, Hinchliffe P (2006) Science 311:1430–1436
Schuler F, Yano T, Di Bernardo S, Yagi T, Yankovskaya V, Singer TP, Casida JE (1999) Proc Natl Acad Sci USA 96:4149–4153
Schulte U, Haupt V, Abelmann A, Fecke W, Brors B, Rasmussen T, Friedrich T, Weiss H (1999) J Mol Biol 292:569–580
Tocilescu MA, Fendel U, Zwicker K, Kerscher S, Brandt U (2007) J Biol Chem 282:29514–29520
Torres-Bacete J, Nakamaru-Ogiso E, Matsuno-Yagi A, Yagi T (2007) J Biol Chem 282:36914–36922
Turrens JF (2003) J Physiol 552:335–344
Verkhovskaya ML, Belevich N, Euro L, Wikström M, Verkhovsky MI (2008) Proc Natl Acad of Sci U S A 105:3763–3767
Vinogradov AD (1998) Biochim Biophys Acta 1364:169–185
Vinogradov AD, Grivennikova VG (2005) Biochemistry (Mosc.) 70:120–127
Vinogradov AD, Sled VD, Burbaev DS, Grivennikova VGX, Moroz IA, Ohnishi T (1995) FEBS Lett 370:83–87
Votyakova TV, Reynolds IJ (2001) J Neurochem 79:266–277
Waletko A, Zwicker K, Abdrakhmanova A, Zickermann V, Brandt U, Kerscher S (2005) J Biol Chem 280:5622–5625
Wikström MKF (1984) FEBS Lett 169:300–304
Yakovlev G, Reda T, Hirst J (2007) Proc Natl Acad Sci U S A 104:12720–12725

Yamaguchi M, Belogrudov G, Hatefi Y (1998) J Biol Chem 273:8094–8098
Yano T, Sklar J, Nakamaru-Ogiso E, Yagi T, Ohnishi T (2003) J Biol Chem 278:15514–15522
Zickermann V, Barquera B, Wikström MKF, Finel M (1998) Biochemistry 37:11792–11796
Zickermann V, Bostina M, Hunte C, Ruiz T, Radermacher M, Brandt U (2003) J Biol Chem 278:29072–29078
Zickermann V, Zwicker K, Tocilescu MA, Kerscher S, Brandt U (2007) Biochim Biophys Acta 1767:393–400
Zwicker K, Galkin A, Dröse S, Grgic L, Kerscher S, Brandt U (2006) J Biol Chem 281:23013–23017